Backstepping multiphase induction machine control impact in presence of open phases fault

Chaker Berrahal, Abderrahim El Fadili
LSIB Laboratory, FST Mohammedia, Hassan II University of Casablanca, Casablanca, Morocco

Article Info	ABSTRACT

As power requirements increase, multiphase induction machines (MPIMs) present a promising alternative to conventional three-phase induction machines. These machines help reduce the current switched by the inverter and circulating through the windings, which in turn mitigates torque ripple. Moreover, incorporating more than three phases enhances system reliability, allowing the machine to maintain operation even in the event of one or more phase failures. This makes MPIMs particularly suitable for high-reliability applications, such as electric vehicles. While most previous studies have concentrated on speed and flux control of MPIMs, less attention has been given to handling open-phase faults. This paper explores the robustness of the backstepping control method applied to MPIMs, particularly in scenarios involving open-phase faults. The proposed multi-loop nonlinear controller is developed to achieve two main objectives: precise speed regulation across a wide range of speed references, and effective rotor flux control. The convergence of the feedback control system is rigorously analyzed using Lyapunov's stability theory. Simulation results show that, although the control objectives are met, stator current demands increase as more phases experience faults. This observation highlights the need for further development of MPIM models that take phase faults into consideration.

Corresponding Author:

Chaker Berrahal
LSIB Laboratory, FST Mohammedia, Hassan II University of Casablanca
Casablanca, Morocco
Email: chaker.berrahal@gmail.com

1. INTRODUCTION

Multiphase induction machines are increasingly popular in industrial applications due to their reliability and high operational availability [1]. The distribution of power across multiple phases results in lower per-phase converter currents, reducing stress on the machine windings and power electronics semiconductors. They offer numerous advantages, including higher torque density, improved torque quality, and increased overall efficiency [2]. This paper aims to provide an overview of the key developments in multiphase induction machines, emphasizing their ability to operate under fault conditions. Extensive research has been conducted on this topic [3], [4], focusing on operational analysis, modeling, control, and fault diagnosis algorithms. As previously mentioned, these machines offer several benefits over their three-phase counterparts [5]. The distribution of power over a greater number of phases reduces electrical and thermal stress per phase, enhancing reliability and power density [6]. Moreover, the increased number of phases provides better operational redundancy, which is valuable in critical applications such as aerospace and electric traction [2], [4]. In the event of a phase failure, the machine can continue operating, albeit with reduced performance, but remains functional [7].

These machines also perform well at low speeds and high torque [7], making them ideal for electric vehicles and renewable energy systems [4], [8]. The renewed interest in multiphase induction machines is supported by advancements in power electronics and advanced control techniques. Control techniques are crucial to fully exploit the characteristics of multiphase induction machines, especially in the presence of faults. These machines differ from conventional three-phase machines in the number of stator phases and are typically powered by multiphase converters, allowing better control and greater operational flexibility. A key feature of multiphase induction machines is their ability to operate in a degraded mode under fault conditions. Thanks to their redundancy and power distribution across multiple phases, these machines can continue functioning, albeit slightly reduced, in the event of one or more phase failures [9]. This is a major advantage for critical applications such as aerospace, marine, and electric traction, where reliability and continuity of service are essential. Several control techniques have been developed for multiphase induction machines, enabling them to operate under normal conditions and in the presence of faults [6], [9]. These include:

- Multivariable vector control [10], [9]: This allows independent control of the machine's torque and flux. This approach is particularly suited to multiphase induction machines due to the complexity associated with the high number of phases.
- Fault-tolerant control strategies [11] : These aim to maintain machine performance even in the event of phase failures. These techniques typically involve reconfiguring the control system to adapt to the new operating conditions .
- Nonlinear control techniques [12]–[14]: Such as backstepping and sliding modes, which offer better performance and greater Impact to disturbances and model uncertainties.

These control approaches have been extensively studied in the literature, demonstrating the potential of multiphase induction machines for critical applications requiring reliability and fault tolerance [15], [16]. The objective of this paper is to present the modeling and control of the integration between a DC/AC converter and a multiphase induction machine connected to a battery. The Impact of the regulator, designed and analyzed using the backstepping technique [17], will be evaluated by introducing faults in one or more arms of the DC/AC converter supplying the multiphase machine. The controller's Impact will be tested through simulations conducted in the MATLAB/Simulink environment [18], [19].

The paper is organized as follows: Section 2 introduces the model of the MultiPhase Induction Machine (MPIM) with n phases and its association with a DC/AC inverter, expressed in the fixed frame (α, β), used to drive a battery-powered electric vehicle. Section 3 is dedicated to the synthesis of a multi-loop nonlinear controller using the backstepping technique and Lyapunov stability. Section 4 presents simulation results to illustrate the control Impact in the event of an open-phase fault.

2. MODELING OF THE SYSTEM

For our study, we consider an n-phase induction machine (MPIM) powered by an n-leg voltage inverter (DC/AC inverter), used to drive a battery-powered electric vehicle. The schematic diagram is shown in Figure 1.

2.1. MPIM model

The model of a MultiPhase induction machine (MPIM) with n phases, expressed in the fixed frame (α, β), was derived using the Park transformation. Using the stator current components ($i_{s\alpha}$ and $i_{s\beta}$) and the rotor flux components ($\phi_{r\alpha}$ and $\phi_{r\beta}$) as state variables, the two-phase model of the MPIM is described by (1).

$$\begin{cases} \frac{d\omega}{dt} & = p\frac{M_{sr}}{JL_r}(\phi_{r\alpha}i_{s\beta} - \phi_{r\beta}i_{s\alpha}) - \frac{T_L}{J} - \frac{f_v}{J}\omega \\ \frac{di_{s\alpha}}{dt} & = -\gamma i_{s\alpha} + \frac{M_{sr}R_r}{\sigma L_s L_r^2}\phi_{r\alpha} + \frac{M_{sr}}{\sigma L_s L_r}p\omega\phi_{r\beta} + \frac{1}{\sigma L_s}v_{s\alpha} \\ \frac{di_{s\beta}}{dt} & = -\gamma i_{s\beta} + \frac{M_{sr}R_r}{\sigma L_s L_r^2}\phi_{r\beta} - \frac{M_{sr}}{\sigma L_s L_r}p\omega\phi_{r\alpha} + \frac{1}{\sigma L_s}v_{s\beta} \\ \frac{d\phi_{r\alpha}}{dt} & = -\frac{R_r}{L_r}\phi_{r\alpha} + p\omega\phi_{r\beta} + \frac{R_r M_{sr}}{L_r}i_{s\alpha} \\ \frac{d\phi_{r\beta}}{dt} & = -\frac{R_r}{L_r}\phi_{r\beta} - p\omega\phi_{r\alpha} + \frac{M_{sr}R_r}{L_r}i_{s\beta} \end{cases} \tag{1}$$

The following notations are used: ($i_{s\alpha}$, $i_{s\beta}$ are stator current $\alpha\beta$ components), ($\phi_{r\alpha}$, $\phi_{r\beta}$ are rotor flux $\alpha\beta$ components),($v_{s\alpha}$, $v_{s\beta}$ are stator voltage $\alpha\beta$ components),(ω is rotor speed, (R_s, R_r are stator and rotor resistances),(L_s, L_r are stator and rotor self-inductances), (M_{sr} is Mutual inductance between the stator and

the rotor), (f_v is friction coefficient,(J is rotor inertia), (T_L is load torque) and (p is the number of pole pairs). with the parameters γ and σ are defined as: $\gamma = \frac{L_r^2 R_s + M_{sr}^2 R_r}{\sigma L_s L_r^2}$ and $\sigma = 1 - \frac{M_{sr}^2}{L_s L_r}$.

2.2. DC/AC inverter model

The modeling of the converter in the multiphase reference frame, shown in Figure 2, involves expressing the voltages at nodes 1, 2, ..., to n of the inverter with respect to the midpoint M. These voltages can be expressed in terms of the switch connection functions and the input voltage as in (2).

$$\begin{bmatrix} v_{S1} \\ v_{S2} \\ . \\ v_{Si} \\ . \\ v_{Sn} \end{bmatrix} = \frac{V_{dc}}{n} \times \begin{bmatrix} (n-1) & -1 & -1 & . & . & -1 \\ -1 & (n-1) & -1 & . & . & -1 \\ . & . & . & . & . & . \\ -1 & -1 & . & (n-1) & . & -1 \\ . & . & . & . & . & . \\ -1 & -1 & -1 & . & . & (n-1) \end{bmatrix} \times \begin{bmatrix} k_1 \\ k_2 \\ . \\ k_i \\ . \\ k_n \end{bmatrix} \tag{2}$$

Where:
- $v_{S1}, v_{S2}, \ldots, v_{Sn}$ are the voltages at nodes 1, 2, ..., to n with respect to the midpoint M.
- $k_1, k_2, \ldots, k_n$ are the switch connection functions (binary variables that take the value 0 or 1).
- V_{dc} is the input voltage (the voltage across the battery).

To simplify this system of (2), we apply the Park transformation. The new system of equations is then represented in the (α, β) reference frame. The inverter is characterized by the independent control of the stator voltage components $v_{s\alpha}$ and $v_{s\beta}$. Accordingly, these voltages are expressed as functions of the corresponding control inputs.

$$\begin{cases} v_{s\alpha} & = V_{dc}.u_1 \\ v_{s\beta} & = V_{dc}.u_2 \end{cases} \tag{3}$$

Where u_1 and u_2 represent the averaged values of the α, β-components within the multiphase duty ratio system, obtained by applying the Park transformation to the duty ratio signals ($k_1,k_2,...,k_n$) and averaging over PWM periods.
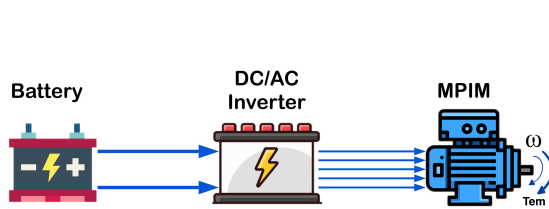

Figure 1. Controlled system
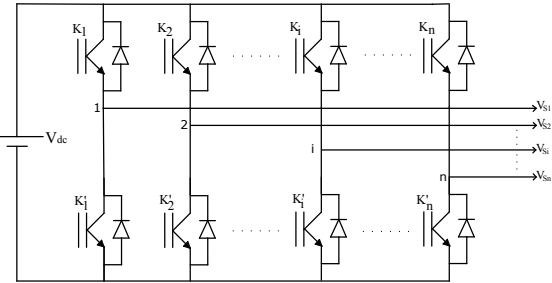

Figure 2. Multiphase DC/AC-inverter

2.3. Modeling of the entire system

Now, let us define the averaged state variables, as in (4).

$$x_1 = \overline{\omega}, x_2 = \bar{i}_{s\alpha}, x_3 = \bar{i}_{s\beta}, x_4 = \overline{\phi}_{r\alpha}, x_5 = \overline{\phi}_{r\beta}, \tag{4}$$

As clear from the context, the notation $\overline{\bullet}$ refers to averaging over the PWM periods. Then, it is proved in many places that instantaneous 'MPIM-inverter association' representation (1) assumes the following averaged form, involving the averaged variables (3) and (4).

$$\dot{x}_1 = -\frac{f_v}{J}x_1 + p\frac{M_{sr}}{L_r}\frac{1}{J}(x_3 x_4 - x_2 x_5) - \frac{T_L}{J} \tag{5}$$

$$\dot{x}_2 = \frac{R_r M_{sr}}{\sigma L_s L_r^2}x_4 + \frac{pM_{sr}}{\sigma L_s L_r}x_5 x_1 - \gamma x_2 + \frac{V_{dc}}{\sigma L_s}u_1 \tag{6}$$

$$\dot{x}_3 = \frac{R_r M_{sr}}{\sigma L_s L_r^2} x_5 - \frac{p M_{sr}}{\sigma L_s L_r} x_4 x_1 - \gamma x_3 + \frac{V_{dc}}{\sigma L_s} u_2 \tag{7}$$

$$\dot{x}_4 = -\frac{R_r}{L_r} x_4 + \frac{R_r}{L_r} M_{sr} x_2 - p\, x_1 x_5 \tag{8}$$

$$\dot{x}_5 = -\frac{R_r}{L_r} x_5 + \frac{R_r}{L_r} M_{sr} x_3 + p\, x_1 x_4 \tag{9}$$

3. CONTROLLER DESIGN
3.1. Control objectives
The operational control objectives are twofold:
- Speed regulation: the machine speed ω must closely follow a given reference signal ω_{ref}.
- Regulating the rotor flux norm $\phi_r = \sqrt{x_4^2 + x_5^2}$ should be maintained at a reference value ϕ_{ref}, ideally equal to its nominal value.

3.2. Motor speed and rotor norm flux control design
The task of controlling the rotor speed and rotor flux norm is now considered for the multiphase induction motor described by (5)-(9). The speed reference $x_1^* = \omega_{ref}$ is any bounded and differentiable function of time, with its first two derivatives being available and bounded. These conditions can always be satisfied by filtering the original (possibly non-differentiable) reference through a unit static gain second-order linear filter. The rotor flux reference ϕ_r is set to its nominal value. The controller design, illustrated in Figure 3 (backstepping control scheme), will be carried out in two steps using the backstepping technique [20]-[23],
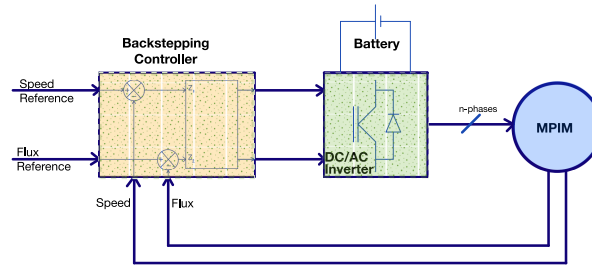

Figure 3. Backstepping control scheme

3.2.1. Step 1: Introducing tracking errors
Let's define the tracking errors as (10) and (11).

$$z_1 = \omega_{ref} - x_1 \tag{10}$$

$$z_2 = \phi_{ref}^2 - (x_4^2 + x_5^2) \tag{11}$$

From (5), (8), and (9), it follows that the errors z_1 and z_2 are governed by the following differential equations, as (12) and (13).

$$z_1 = \dot{\omega}_{ref} + \frac{f_v x_1}{J} - \frac{p M_{sr}}{J.L_r}(x_3 x_4 - x_2 x_5) + \frac{T_L}{J} \tag{12}$$

$$z_2 = 2\phi_{ref}\dot{\phi}_{ref} - \frac{2R_r M_{sr}}{L_r}(x_2 x_4 + x_3 x_5) + \frac{2R_r}{L_r}(\phi_{ref}^2 - z_2) \tag{13}$$

In (12) and (13), the terms $p\frac{M_{sr}}{JL_s}(x_3 x_4 - x_2 x_5)$ and $\frac{2R_r M_{sr}}{L_r}(x_2 x_4 + x_3 x_5)$ emerge as virtual control signals. Were these actual control signals, the error system (12) and (13) could be globally asymptotically stabilized by setting $p\frac{M_{sr}}{JL_s}(x_3 x_4 - x_2 x_5) = \mu_1$ and $\frac{2R_r M_{sr}}{L_r}(x_2 x_4 + x_3 x_5) = \nu_1$, where:

$$\mu_1 \overset{def}{=} (c_1 z_1 + \dot{\omega}_{ref}) + \frac{T_L}{J} + \frac{f_v}{J}(\omega_{ref} - z_1) \tag{14}$$

$$\nu_1 \overset{def}{=} c_2 z_2 + 2\phi_{ref}\dot{\phi}_{ref} + 2\frac{R_r}{L_r}(\phi_{ref}^2 - z_2) \tag{15}$$

Here, c_1 and c_2 represent positive design parameters. However, since $p\frac{M_{sr}}{JL_s}(x_3 x_4 - x_2 x_5)$ and $\frac{2R_r M_{sr}}{L_r}(x_2 x_4 + x_3 x_5)$ are not the actual control signals, they cannot be equated to μ_1 and ν_1 respectively. Nonetheless, we retain the expressions of μ_1 and ν_1 as initial stabilizing functions and introduce the new errors [23]-[25].

$$z_3 = \mu_1 - p\frac{M_{sr}}{J.L_r}(x_3 x_4 - x_2 x_5) \tag{16}$$

$$z_4 = \nu_1 - 2\frac{R_r}{L_r}M_{sr}(x_2 x_4 + x_3 x_5) \tag{17}$$

Then, using the notations (10)-(17), the dynamics of the errors z_1 and z_2, initially described by (12) and (13), can be rewritten as (18) and (19).

$$z_1 = -c_1 z_1 + z_3 \tag{18}$$

$$z_2 = -c_2 z_2 + z_4 \tag{19}$$

3.2.2. Step 2: Deriving control signals
To ensure the convergence of all errors (z_1, z_2, z_3, z_4) to zero, we need to elucidate the dependency of these errors on the actual control signals (u_1, u_2). Initially focusing on z_3, we derive its dynamics from (16).

$$z_3 = \dot{\mu}_1 - p\frac{M_{sr}}{JL_r}(\dot{x}_3 x_4 + x_3 \dot{x}_4 - \dot{x}_2 x_5 - x_2 \dot{x}_5) \tag{20}$$

Utilizing (5)-(9) and (14), we simplify (20) to (21).

$$z_3 = \mu_2 - p\frac{M_{sr}}{JL_r}\frac{V_{dc}}{\sigma L_s}(x_5 u_1 - x_4 u_2) \tag{21}$$

Where, as in (22).

$$\mu_2 = \left[c_1(-c_1 z_1 + z_3) + \ddot{\omega}_{ref} + \frac{\dot{T_L}}{J} - \frac{f_v . T_L}{J^2}\right] + \frac{pM_{sr}}{J.L_r}(\frac{f_v}{J} + \frac{R_r}{L_r} + \gamma)(x_4 x_3 - x_2 x_5)$$

$$+ \frac{p^2 M_{sr} x_1}{J.L_r}(x_3 x_5 + x_2 x_4) + p^2 \frac{M_{sr}^2}{\sigma J.L_s L_r^2}x_1(x_4^2 + x_5^2) \tag{22}$$

Similarly, for z_4 from (17), we have (23).

$$z_4 = \dot{\nu}_1 - \frac{2R_r M_{sr}}{L_r}(\dot{x}_2 x_4 + x_2 \dot{x}_4 + \dot{x}_3 x_5 + x_3 \dot{x}_5) \tag{23}$$

Substituting (5)-(9) and (15) into (23), we get (24).

$$z_4 = \nu_2 - 2\frac{R_r}{L_r}M_{sr}\frac{V_{dc}}{\sigma L_s}(u_1 x_4 + u_2 x_5) \tag{24}$$

Where, as in (25).

$$\nu_2 = c_2(-c_2 z_2 + z_4) + 2(\dot{\phi}_{ref}^2 + \phi_{ref}\ddot{\phi}_{ref}) - (2(\frac{R_r}{L_r})^2 + 2(\frac{R_r}{L_r})^2 \frac{M_{sr}}{\sigma L_s L_r}M_{sr})(x_4^2 + x_5^2)$$

$$-2(\frac{R_r M_{sr}}{L_r})^2(x_2^2+x_3^2)+\frac{2pR_r M_{sr}}{L_r}x_1(x_2 x_5 - x_3 x_4)+(4(\frac{R_r}{L_r})^2 M_{sr}+2\frac{R_r}{L_r}\gamma M_{sr})(x_2 x_4 + x_3 x_5) \quad (25)$$

Now, considering the error system (18)-(19), (21), and (24), we propose an augmented Lyapunov function candidate.

$$V = \frac{1}{2}z_1^2 + \frac{1}{2}z_2^2 + \frac{1}{2}z_3^2 + \frac{1}{2}z_4^2 \quad (26)$$

Its time-derivative along the trajectory of the state vector (z_1, z_2, z_3, z_4) is as (27).

$$V = \dot{z}_1 z_1 + \dot{z}_2 z_2 + \dot{z}_3 z_3 + \dot{z}_4 z_4 \quad (27)$$

Utilizing (18)-(19), (21), (24), and (27) expands as (28).

$$V = z_1(-c_1 z_1 + z_3) + z_2(-c_2 z_2 + z_4) + z_3(\mu_2 - \frac{pM_{sr}V_{dc}}{\sigma L_s L_r}(x_5 u_1 - x_4 u_2))$$

$$+z_4(\nu_2 - 2\frac{R_r M_{sr}V_{dc}}{\sigma L_s L_r}(x_4 u_1 + x_5 u_2)) \quad (28)$$

Supplementing $c_3 z_3^2 - c_3 z_3^2 + c_4 z_4^2 - c_4 z_4^2$ to the right side of (28) and rearranging terms, we obtain (29).

$$V = -c_1 z_1^2 - c_2 z_2^2 - c_3 z_3^2 - c_4 z_4^2$$
$$+z_3\left[\mu_2 + z_1 + c_3 z_3 - \frac{pM_{sr}V_{dc}}{\sigma L_s L_r}(x_5 u_1 - x_4 u_2)\right]$$
$$+z_4\left[c_4 z_4 + z_2 + \nu_2 - 2\frac{R_r M_{sr}V_{dc}}{\sigma L_s L_r}(x_4 u_1 + x_5 u_2)\right] \quad (29)$$

Here, c_3 and c_4 represent new positive real design parameters. (29) implies that the control signals u_1, u_2 must be selected to render the quantities within the curly brackets on the right side of (29) to zero. Setting these quantities to zero and solving the resulting second-order linear equation system with respect to (u_1, u_2) yields the following control law, as in (30).

$$\begin{bmatrix} u_1 \\ u_2 \end{bmatrix} = \begin{bmatrix} \lambda_0 & \lambda_1 \\ \lambda_2 & \lambda_3 \end{bmatrix}^{-1} \begin{bmatrix} z_1 + c_3 z_3 + \mu_2 \\ z_2 + c_4 z_4 + \nu_2 \end{bmatrix} \quad (30)$$

With:

$$\lambda_0 = p\frac{V_{dc}}{\sigma L_s}\frac{M_{sr}}{L_r}x_5, \lambda_1 = -p\frac{V_{dc}}{\sigma L_s}\frac{M_{sr}}{L_r}x_4$$

$$\lambda_2 = 2R_r \frac{V_{dc}}{\sigma L_s}\frac{M_{sr}}{L_r}x_4, \lambda_3 = 2R_r \frac{V_{dc}}{\sigma L_s}\frac{M_{sr}}{L_r}x_5 \quad (31)$$

Notably, the matrix $\begin{bmatrix} \lambda_0 & \lambda_1 \\ \lambda_2 & \lambda_3 \end{bmatrix}$ is nonsingular, as its determinant, $D = \lambda_0 \lambda_3 - \lambda_2 \lambda_4 = -2\frac{R_r}{L_r}\frac{V_{dc}}{\sigma L_s}M_{sr}(x_4^2 + x_5^2)$, remains non-zero since the flux $\phi_r = \sqrt{x_4^2 + x_5^2}$ never vanishes practically due to the presence of the remnant flux. Substituting the control law (30) into (u_1, u_2) on the right side of (29), we get (32).

$$V = -c_1 z_1^2 - c_2 z_2^2 - c_3 z_3^2 - c_4 z_4^2 \quad (32)$$

Since the right side of (32) is a negative definite function of the state vector (z_1, z_2, z_3, z_4), the latter globally asymptotically vanish [14]. This result is more explicitly formulated in the following theorem:

Theorem: stability and convergence analysis: consider the closed-loop system comprising:

  − The MPIM-DC/AC converter association, described by model (5)-(9)
  − The nonlinear controller defined by the control law (30)

Then, the following properties hold:
  − The closed-loop error system, expressed in the (z_1, z_2, z_3, z_4) coordinates, evolves according to (33)-(36).

$$z_1 = -c_1 z_1 + z_3 \tag{33}$$

$$z_2 = -c_2 z_2 + z_4 \tag{34}$$

$$z_3 = -c_3 z_3 - z_1 \tag{35}$$

$$z_4 = -c_4 z_4 - z_2 \tag{36}$$

  − The above linear system is stable with respect to the Lyapunov function $V = \frac{1}{2}z_1^2 + \frac{1}{2}z_2^2 + \frac{1}{2}z_3^2 + \frac{1}{2}z_4^2$, and the errors (z_1, z_2, z_3, z_4) exponentially converge to zero.

Proof: (33) and (34) directly stem from (18)-(19). (35) is derived by substituting the control law (30) into (u_1, u_2) on the right side of (21). Similarly, (36) is obtained by substituting the control law (30) into (u_1, u_2) on the right side of (24). Thus, Part 1 is established. Furthermore, from (26), it is evident that $V = \frac{1}{2}z_1^2 + \frac{1}{2}z_2^2 + \frac{1}{2}z_3^2 + \frac{1}{2}z_4^2$ serves as a (radially unbounded) Lyapunov function for the error system (33)-(36). Since $\dot{V}$ is a semi-negative definite function of the state vector (z_1, z_2, z_3, z_4), by Lyapunov's equilibrium point theorem, the entire error system is exponentially asymptotically stable, and the errors converge to zero.

4.   SIMULATION AND RESULTS

The control system, described by model (5)-(9), and the control law (30), are evaluated via simulation. The system's characteristics are summarized in Table 1. The Impact of the backstepping multiphase induction machine control is assessed both with and without open phase faults. The machine load remains constant, and the MPIM operates at a high speed ($\omega_{ref} = 100 rd/s$). Initially, the machine operates without open phase faults over the interval $[0, 10s]$. At $t = 10s$, an open fault occurs in phase number one, and another fault occurs in phase number four at $t = 14s$. The reference value Φ_r for the rotor flux norm is set to its nominal value ($1wb$). The indicated values of design parameters c_1, c_2, c_3, c_4 have been selected using a 'try-and-error' search method and proved to be suitable. The experimental setup is simulated within the MATLAB/Simulink environment with a calculation step of $5\mu s$. This value is chosen considering that the inverter frequency commutation is 15 kHz.

Table 1. System features

Feature	Symbole	Value	Unit
Induction machine			
Nominal power	P_n	7.5	kW
Nominal current	I_n	9.6	A
Stator resistance	R_s	0.63	Ω
Stator cyclic inductance	L_s	0.098	H
Rotor resistance	R_r	0.40	Ω
Rotor cyclic inductance	L_r	0.09	H
Mutual inductance	M_{sr}	0.09	H
Inertia	J	0.22	$kg.m^2$
Viscous rubbing	f_v	0.001	$Nm/rd/s$
Number of pole pairs	p	2	
Number of phases	n	5	
DC-AC converter			
Continuous voltage Bus	V_{dc}	500	V
PWM frequency	F_m	15.00	kHz

The control performance obtained is depicted in Figures 4-8, illustrating the impact of nonlinear backstepping control against one or two phase failure faults on one or two supply phases, respectively, of the multiphase induction machine. Initially, the MPIM operates without any fault until $t = 10$ s. At $t = 10$ s, the first

open phase fault occurs in phase number one, followed by a second fault simultaneously in phase number four, starting from $t = 14$ s. Figures 4-8 demonstrate the responses of rotor speed, rotor flux, the phase stator current unaffected by any fault, and electromagnetic torque. For both controlled variables (ω, Φ_r), the tracking quality is highly satisfactory across all speed ranges (refer to Figures 4 and 5). In both scenarios, the rotor flux norm and rotor speed closely match their references and converge to them after the occurrence of each fault. Remarkably, even in the presence of a single or double fault, the motor speed and the rotor flux converge towards their references. Figure 7 illustrates the electromagnetic torque generated by the multiphase induction machine before and after the occurrence of open-phase faults. The machine is loaded with a constant torque T_l set at $20 N.m$. Initially, without any faults, the electromagnetic torque converges, following a transient state, towards $20 N.m$. The slight torque ripples observed in Figure 7 stem from the power supply of the MPIM by the DC/AC converter. After the first open-phase fault, the average value of the electromagnetic torque remains unchanged, but the amplitude of the ripples increases by 10%. This increase further intensifies with the presence of two simultaneous open-phase faults, reaching up to 40% (as depicted in Figure 8).
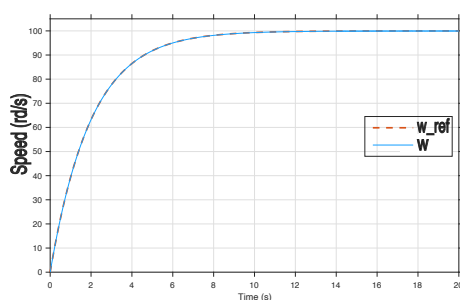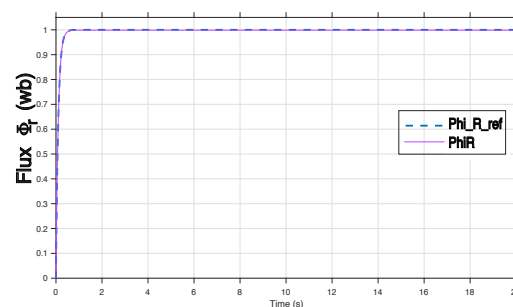

Figure 4. Rotor speed response
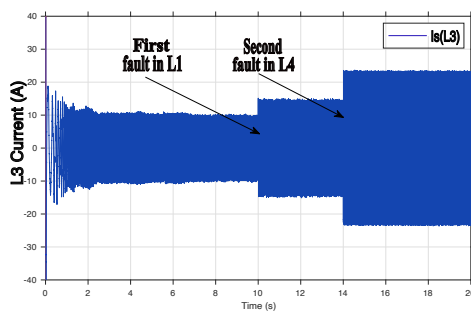

Figure 5. Rotor Flux response

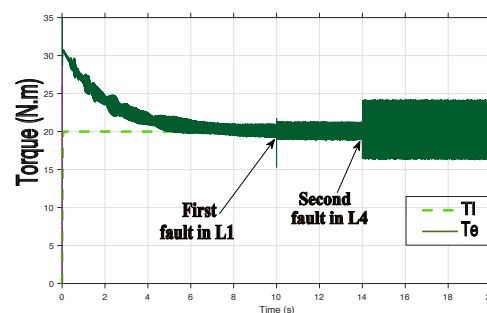Figure 6. Stator current in phase number 3 response
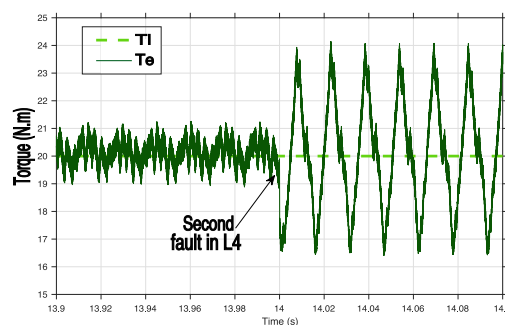

Figure 7. Electromagnetic torque response

Figure 8. Zoom in electromagnetic torque

In Figure 6, the stator current absorbed by phase number 3, the phase unaffected by any faults, is depicted. At the onset of a single open phase fault at $t = 10$s, the stator current of phase number 3 surges by 50% compared to its value in the absence of a fault. With the occurrence of two simultaneous open phase faults starting from $t = 14$s, affecting phases number 1 and number 4, this current escalates by over 150%.

5.   CONCLUSION

This study explores the impact of backstepping control for multiphase induction machines in the presence of open-phase faults. The controller was designed and analyzed using the backstepping technique, integrating the multiphase induction machine and the DC/AC inverter modeled in the fixed frame (α, β), without considering open-phase faults. The proposed controller incorporates nonlinear loops aimed at ensuring precise regulation of rotor speed and flux. The impact of backstepping control was evaluated in single and double open-phase fault scenarios. In both cases, the rotor flux norm and rotor speed closely followed their references, converging to them after each fault event. Even in the presence of open-phase faults, the motor speed and rotor flux converged to their references. After the occurrence of open-phase faults, the stator current absorbed by the non-faulty phases increased by 50% and 150%, respectively. Although the electromagnetic torque generated by the multiphase induction machine maintained the average value of the load torque after open-phase faults, the ripple amplitude increased by 40%. Hence, the design and analysis of backstepping control must consider the presence of open-phase faults.

REFERENCES

[1]   E. Levi, "Multiphase electric machines for variable-speed applications," *IEEE Transactions on Industrial Electronics*, vol. 55, no. 5, pp. 1893–1909, May 2008, doi: 10.1109/tie.2008.918488.

[2]   F. Barrero and M. J. Duran, "Recent advances in the design, modeling, and control of multiphase machines—Part I," *IEEE Transactions on Industrial Electronics*, vol. 63, no. 1, pp. 449-458, Jan. 2016, doi: 10.1109/TIE.2015.2447733.

[3]   F. Giri, "AC electric motors control: advanced design techniques and applications," John Wiley & Sons, 2013, doi: 10.1002/9781118574263.

[4]   M. Cheng, P. Han, G. Buja, and M. G. Jovanovi´c, "Emerging multiport electrical machines and systems: Past developments, current challenges, and future prospects," *IEEE Transactions on Industrial Electronics*, vol. 65, no. 7, pp. 5422-5435, 2018, doi: 10.1109/tie.2017.2777388.

[5]   O. Dordevic, N. Bodo, and M. Jones, "Model of an induction machine with an arbitrary phase number in MATLAB/Simulink for educational use," in *Proceedings of the 2010 IEEE International Conference*, 2010, pp. 1-6, doi: 10.1109/iecon.2017.8217403.

[6]   C. Carunaiselvane and T. R. Chelliah, "Present trends and future prospects of asynchronous machines in renewable energy systems," *Renewable & Sustainable Energy Reviews*, vol. 74, pp. 1028–1041, 2017, doi: 10.1016/j.rser.2016.11.069.

[7]   B. D. S. G. Vidanalage, S. Mukundan, W. Li, and N. C. Kar, "An overview of pm synchronous machine design solutions for enhanced traction performance," in *2020 International Conference on Electrical Machines (ICEM)*, IEEE, 2020, vol. 1, pp. 1697–1703, doi: 10.1109/icem49940.2020.9270882.

[8]   M. J. Dur´an and F. Barrero, "Recent advances in the design, modeling, and control of multiphase machines—Part II," *IEEE Transactions on Industrial Electronics*, vol. 63, no. 1, pp. 459-468, Jan. 2016, doi: 10.1109/TIE.2015.2448211.

[9]   H. A. Toliyat and T. A. Lipo, "Analysis of concentrated winding induction machines for adjustable speed drive applications-experimental results," *IEEE Transactions on Energy Conversion*, vol. 9, no. 4, pp. 695–700, 1994, doi: 10.1109/60.368339.

[10]   M. P. Razafindraibe and P. A. Randriamitantsoa, "Multivariable control of the three-phase asynchronous 'cage' motor by variation frequency (in French: Commande multivariable du moteur asynchrone triphas´e 'a cage par variation de fr´equence)," Technical report, 2010.

[11]   L. Frosini, "Novel diagnostic techniques for rotating electrical machines—A review," *Energies*, vol. 13, no. 19, p. 5066, 2020, doi: 10.3390/en13195066.

[12]   Z. Peng, Z. Zheng, Y. Li, and Z. Liu, "Fault-tolerant control of multiphase induction machine drives based on virtual winding method," in *2017 IEEE Transportation Electrification Conference and Expo (ITEC)*, IEEE, 2017, pp. 252–256, doi: 10.1109/itec.2017.7993280.

[13]   C. Berrahal, A. E. Fadili, F. Giri, A. E. Magri, R. Lajouad, and I. E. Myasse, "Robustness of backstepping multiphase induction machine control in presence of open phases fault," *IFAC-PapersOnLine*, vol. 55, no. 12, pp. 794-799, Aug. 2022, doi: 10.1016/j.ifacol.2022.07.410.

[14]   K. Saad, K. Abdellah, H. Ahmed, and A. Iqbal, "Investigation on svm-backstepping sensorless control of five-phase open-end winding induction motor based on model reference adaptive system and parameter estimation," *Engineering Science and Technology, an International Journal*, vol. 22, no. 4, pp. 1013-1026, 2019, doi: 10.1016/j.jestch.2019.02.008.

[15]   F. J. Lin, C. K. Chang, and P. K. Huang, "FPGA-based adaptive backstepping sliding-mode control for linear induction motor drive," *IEEE Transactions on Power Electronics*, vol. 22, no. 4, pp. 1222-1231, 2007, doi: 10.1109/tpel.2007.900553.

[16]   T. K. Tleugaliuly, "The multi-motor asynchronous electric drive of the coordinated rotation in case of asymmetrical power supply," in *2019 International Multi-Conference on Industrial Engineering and Modern Technologies (FarEastCon)*, pp. 1–5, 2019, doi: 10.1109/fareastcon.2019.8934374.

[17]   H. K. Khalil, "Nonlinear systems," Prentice Hall, 3rd ed., 2002.

[18] H. Ouadi, F. Giri, A. Elfadili, and L. Dugard, "Induction machine speed control with flux optimization," *Control Engineering Practice*, vol. 18, no. 1, pp. 55–66, 2010, doi: 10.1016/j.conengprac.2009.08.006.

[19] R. Lajouad, A. El Magri, and A. El Fadili, "Robust adaptive nonlinear controller of wind energy conversion system based on permanent magnet synchronous generator," in *Renewable Energy Systems*, Academic Press, 2021, pp. 133-159, doi: 10.1016/B978-0-12-820004-9.00001-2.

[20] A. El Fadili, F. Giri, A. El Magri, L. Dugard, and F. Z. Chaoui, "Adaptive nonlinear control of induction motors through AC/DC/AC converters," *Asian Journal of Control*, vol. 14, no. 6 pp. 1470–1483, 2012, doi: 10.3182/20130703-3-fr-4038.00040.

[21] A. Elfadili, F. Giri, H. Ouadi, A. El Magri, and A. Abouloifa, "Induction motor control through AC/DC/AC converters," in *Proceedings of the 2010 American Control Conference*, 2010, pp. 1755–1760, doi: 10.1109/acc.2010.5531480.

[22] I. Drhorhi *et al.*, "Adaptive backstepping controller for DFIG-based wind energy conversion system," in *Backstepping control of nonlinear dynamical systems*, Academic Press, 2021, pp. 235-260, doi: 10.1016/B978-0-12-817582-8.00018-0.

[23] I. El Myasse, A. El Magri, M. Kissaoui, R. Lajouad, and C. Berrahal, "Adaptive nonlinear control of generator load VSC-HVDC association," *IFAC-PapersOnLine*, vol. 55, no. 12, pp. 782-787, 2022, doi: 10.1016/j.ifacol.2022.07.408.

[24] S. Gheouany, H. Ouadi, C. Berrahal, S. El Bakali, J. El Bakkouri, and F. Giri, "Multi-stage energy management system based on stochastic optimization and extremum-seeking adaptation," *IFAC-PapersOnLine*, vol. 56, no. 2, pp. 5457-5462, 2023, doi: 10.1016/j.ifacol.2023.10.197.

[25] A. El Fadili, F. Giri, A. El Magri, R. Lajouad, and F. Z. Chaoui, "Adaptive control strategy with flux reference optimization for sensorless induction motors," *Control Engineering Practice*, vol. 26, pp. 91–106, 2014, doi: 10.1016/j.conengprac.2013.12.005.

BIOGRAPHIES OF AUTHORS

Chaker Berrahal was born in 1976. He received the Aggregation of Electrical Engineering from the Ecole Normale Supérieure de l'Enseignement Technique, (ENSET), Rabat, Morocco, in 2000. He received a Master degree in "Electrical Engineering" from École Nationale Supérieure d'Arts et Métiers (ENSEM), Rabat, Morocco, in 2018, with over 20 years of experience teaching industrial maintenance at the Higher Technical Certificate (BTS) level. He currently teaches at IBN SINA Technical High School in Kenitra, Morocco, where he also serves as the president of the national jury for the BTS in Industrial Maintenance. His research focuses on the nonlinear control of Multiphase Induction machines. Additionally, he has played a key role in developing the BTS Industrial Maintenance curriculum, contributing to international educational cooperation between Morocco, France, and Canada. He can be contacted at email: chaker.berrahal@gmail.com.

Abderrahim El Fadili was born in 1974. He received the Aggregation of Electrical Engineering from the Ecole Normale Supérieure de l'Enseignement Technique, (ENSET), Rabat, Morocco, in 2001, the Ph.D. degree in control engineering from the Mohammed V University, Rabat, Morocco, in 2011. Currently, he is a Professor at the Faculty of Sciences and Techniques of Mohammedia, Hassan II University of Casablanca, Morocco since 2015. His research interests include adaptive and robust non-linear control and optimization, system stability study of non-linear systems, synthesis of non-linear observers, and discretization and discrete control of non-linear systems. He has published over 60 journal/conference papers on these topics. He can be contacted at email: elfadili_abderrahim@yahoo.fr.